

Tar conversion of biomass syngas in a downstream char bed

D. Fuentes-Cano^a, L. von Berg^b, A. Diéguez-Alonso^c, R. Scharler^b, A. Gómez-Barea^a, A. Anca-Couce^b

^a Chemical and Environmental Engineering Department, University of Seville, Camino de los Descubrimientos s/n, 41092 Seville, Spain

^b Institute of Thermal Engineering, Graz University of Technology, Inffeldgasse 25b, Graz, 8010, Austria

^c Technische Universität Berlin, Institute of Energy Engineering, Chair for Energy Process Engineering and Conversion Technologies for Renewable Energies, Seestr. 13, 13353 Berlin, Germany

Abstract

The catalytic conversion of biomass-derived tars over char during long tests (over 6 hours) is studied. The syngas is generated in a steam-blown fluidized-bed gasifier employing wood pellets and conducted to a second tubular reactor where non-activated char particles are fluidized. The gasifier operated at 750 °C whereas the temperature of the secondary reactor was varied between 750 °C and 875 °C. The evolution of the tar conversion, gas composition and internal structure of the used catalysts were studied. At 750 °C, the initial catalytic activity of the char was low and deactivation occurs rapidly. However, as the reactor temperature increased, the catalytic activity of the char improved significantly. At 875 °C, the initial conversion of tar was above 70 % and over 64 % after 5 h of operation. Moreover, the conversion of the heaviest tars was above 80 % during the entire test. At this temperature, the decrease in tar conversion is attributed to the consumption of the char by steam gasification since its catalytic activity increased during of the test. In these conditions the char bed with an initial weight of 32 g converted approximately 12 g of tars (benzene not included) after 5 h of operation.

1- Introduction

Gasification is a thermo-chemical route for conversion of solid fuels, such as biomass and wastes, into a syngas that can be used in a variety of applications [1,2]. Fluidized bed (FB) gasification has several advantages over that in fixed/moving bed or entrained-flow for distributed energy production [3]. However, in all types of FB gasifiers the process temperature must be kept relatively low to prevent agglomeration and sintering of bed material. The low temperature results in incomplete carbon conversion and a high concentration of heavy tars in the gas. The condensation of heavy tars in downstream equipment is the main bottleneck for the use of the syngas in any application where the gas needs to be cooled down.

During the last decades, different methods have been developed to reduce the tar concentration in the gas based on physical separation (wet/physical methods) or reforming/cracking of the tar in the hot gas. Wet methods have been tested using water [4,5] or organic solvents [6], and have been reported to be technically efficient. However, this way to clean the gas seems to be too complex and expensive for small or medium-size plants [1]. The reforming/cracking of tar using metallic catalysts (mainly Ni-based) in a downstream vessel is also efficient [7,8] but the presence of certain contaminants in the syngas causes their rapid deactivation. The fast

43 deactivation by poisoning or coking and the relatively high price of metallic-based catalysts have
44 driven the search for alternative catalysts such as olivine, dolomite, alkali-catalysts and char
45 [7,9].

46 Char presents several advantages over traditional catalysts [10]. Char is a byproduct from the
47 process (pyrolysis or gasification), therefore it is available and cheap unless special treatment is
48 required for its activation; it is relatively resistant to poisoning by sulfur and chlorine and it can
49 be burnt once used. Additionally, according with the results of different works, char converts
50 preferentially the heavier compounds of the tar mixture [10-12]. This is a significant advantage
51 when the aim is to reduce the tar dew point of the gas (so that it can be burned in an engine) as
52 it is mainly determined by the concentration of polyaromatic compounds. However, char may
53 deactivate rapidly due to coking under some operating conditions [10,13-15].

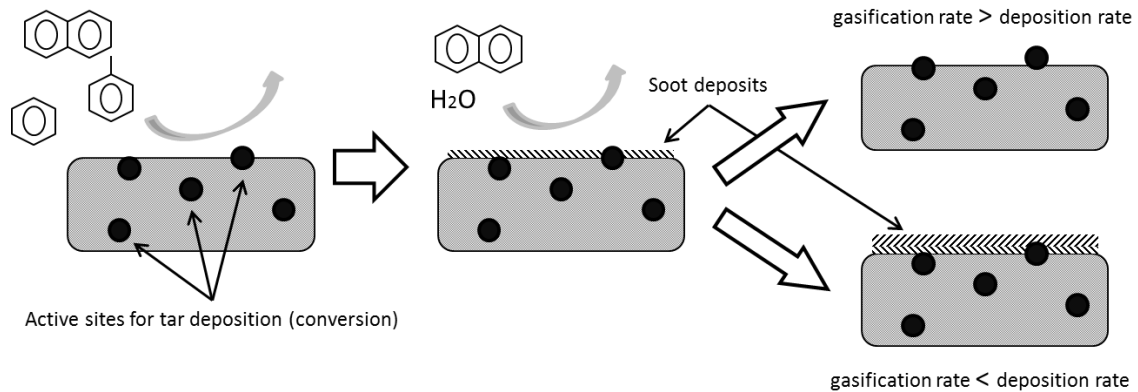
54 The Viking staged gasifier, developed at the Technical University of Denmark, produces the
55 pyrolysis of wood chips in a screw conveyor to, subsequently, partially oxidize the gas either
56 with air [11,16] or with O₂/CO₂ [17] mixtures. After oxidation, the gas, at temperatures as high
57 as 1200 °C, is transferred to a fixed bed of the char produced during pyrolysis. This configuration,
58 has demonstrated to convert most of the heavy tars present in the syngas, although it is difficult
59 to scale up. A different system, the FLETGAS process [3], would convert most of the heavy tar in
60 the syngas using a secondary char bed while improving the scalability of the system due to the
61 use of fluidized beds.

62 The catalytic activity of char and activated carbons depends on the amount and chemical
63 composition of the surface available for tar reaction [18-19]. Both parameters depend, in turn,
64 on the original parent material and the severity (temperature and gas residence time) of the
65 activation process. Non-activated chars typically present total surface areas below 300 m²/g
66 while this value can increase above 1000 m²/g after activation [20]. However, a significant
67 portion of this area could be non-accessible for the conversion of large molecules, such as
68 naphthalene (kinetic diameter 0.74 nm [21]), due to diffusional limitations in narrow micropores
69 (internal diameter below 2 nm) and pore mouth blocking [18].

70 The presence of different functional groups, such as oxo-groups (-CO, -COH or -COOH) or alkali
71 and alkaline earth metals (AAEM), distributed over the char surface has been reported to be
72 responsible for its high activity towards tar conversion [18-20,22-24]. According to the results
73 presented by Feng et al. [25], the activation process either with H₂O or with CO₂ not only
74 increases the concentration of surface oxo-groups but also promotes the migration of AAEM
75 species from the char matrix to the char surface, creating carbon-metal complexes, which
76 increase the catalytic activity of the char surface. A recent publication suggests the presence of
77 two different types of surface in the original char [26]. The first type would be responsible for
78 the initial high activity of the catalyst towards tar conversion but, in absence of gasification
79 agents, its deactivation occurs rapidly. The second type of surface would present a lower activity
80 but its deactivation, if occurs, is much slower.

81 Fig. 1 presents a simplified scheme of the tar conversion mechanism over char. The tar
82 compound in the syngas reacts with the functional groups, or active sites, dispersed on the char
83 surface. At sufficiently high temperature [27-29] the adsorbed tar compound undergoes
84 polymerization, creating a soot/coke deposit over the original char surface [13,15]. The
85 reactivity of the soot deposit is much lower towards steam gasification [30,31] and towards
86 catalytic tar conversion [13,15] than the original char surface. Therefore, if the soot gasification
87 rate is lower than the soot deposition rate, the original char surface gets covered by soot, the

88 total surface area decreases and, consequently, the activity of the char diminishes with time. On
89 the contrary, when gasification is faster than deposition, the char can maintain or even increase
90 its initial activity. Therefore, the selection of experimental conditions ensuring a positive net rate
91 of carbon conversion (gasification – deposition) is necessary to maintain the activity of the char
92 [10,13-15,30].



93

94 Figure 1: Tar conversion mechanism over char. Reprinted from [13]

95 Most of the studies analyzing tar conversion over char have been conducted using a simulated
96 syngas doped with model tars instead of using a real gasification gas. The use of simulated (and
97 simplified) syngas as surrogate syngas is convenient when a careful control of experimental
98 conditions is necessary to isolate processes and investigate detailed aspects of mechanisms of
99 conversion. However, the use of real pyrolysis/gasification gas containing dozens/hundreds of
100 different compounds is more useful to verify the activity of char in a real gasification process
101 since the competition between different tar compounds for the active sites can influence their
102 conversion [32]. Matsuhara et al. [15] studied the conversion of a coal pyrolysis gas over a fixed
103 bed of char produced by pyrolysing the same coal. A significant improvement on the tar
104 conversion was measured when the char bed temperature was increased from 750 °C to 900 °C.
105 In spite of the relatively low gas spatial velocity (gas flowrate, divided by the mass of char in the
106 bed) a significant char deactivation was observed during the first 20 minutes of test. However,
107 at the highest temperature tested (900 °C), a net carbon consumption was reported and no
108 significant deactivation of the char bed was detected after 40 min of test.

109 The present paper aims at investigating the technical viability of using non-activated biomass
110 char for tar conversion. For this purpose, a real gasification gas has been produced in a steam
111 blown bubbling fluidized bed reactor operated at 750 °C using wood pellets as fuel. The syngas
112 produced was then treated at temperatures between 750 °C and 875 °C in a secondary fluidized
113 bed reactor filled with non-activated char particles produced by beech wood pyrolysis. The
114 process is maintained for times over 6 hours to track the evolution of the char activity towards
115 tar catalytic conversion. Both the evolution of the syngas composition (including light gases and
116 tar compounds) and the characteristics of the spent chars (after used) are reported.

117

118 2- Experimental

119

120 2.1- Materials

121 2.1.1- Biomass

122 Spruce wood pellets with a diameter of 6 mm and a length of about three times the diameter
 123 were used as feedstock in the FB gasifier. The elemental composition and ash content in dry
 124 basis of the pellets are shown in Table 1. The moisture content was of 7% w.b. CHNS content
 125 was determined in an elemental analyzer (Elementar Vario EL-III). The ash content was
 126 determined by DIN norm 51719. The content of inorganic species was measured by ICP-OES
 127 (Varian 720-ES) after digestion in a microwave with H₂O₂ and HNO₃.

128 Table 1: Ultimate analysis and elemental analysis of ashes of the different materials used.

	C	H	N	S	O	Ash	Fe	Mg	Na	P	Ca	K
	(wt.%, dry basis)						mg/kg (dry basis)					
Wood pellets – FB gasifier	49.5 ±0.1	6.6 ±0.1	0.1 ±0.0	0.1 ±0.1	43.5 ±0.1	0.3	30.1 ±1.0	150.4 ±4.1	13.2 ±0.4	49.8 ±1.3	1025 ±30	341.0 ±21.3
Char from beech wood chips	88.3 ±0.3	1.8 ±0.0	0.3 ±0.0	0.1 ±0.0	6.4 ±0.3	3.1	131.7 ±6.8	1854 ±89	245.3 ±13.5	500.8 ±16.2	8330 ±383	6065 ±180

129

130 2.1.2- Char

131 The char used in the secondary reactor was produced via slow pyrolysis of beech wood chips in
 132 a N₂ atmosphere in a two-step process. First, the beech wood was pyrolyzed at approximately
 133 450 °C in a N₂ blown continuous screw reactor. The retention time of the biomass/char in the
 134 reactor was 30 min. In a second step, the char was subjected to pyrolysis at 700 °C (measured in
 135 the center of the bed) in a semi-batch fixed-bed reactor (batch bed of char with continuous flow
 136 of N₂). The time required to heat the char from ambient temperature to 700 °C was 1 h and the
 137 char was then kept for one more hour at 700 °C. The elemental composition and ash content in
 138 dry basis of the fresh char employed in the experiments are shown in Table 1.

139 2.2- Test rig

140 The tests were performed using the syngas produced in a lab-scale FB biomass gasifier. This
 141 syngas was fed to a secondary FB reactor filled with char in order to investigate the tar
 142 conversion and the deactivation behavior of the char. Fig. 2 presents the flowchart of the
 143 experimental set-up.

144 2.2.1- Fluidized bed gasifier

145 The fluidized bed reactor was heated by an electrical oven in order to keep the bed temperature
 146 constant at 750 °C. The reactor was made of stainless steel and had an inner diameter of 80 mm
 147 and a height of 150 mm at the bottom-part, while the freeboard region consisted of a conical
 148 part of 80 mm height where the inner diameter opens up to 250 mm followed by a cylindrical
 149 part of 110 mm of height. 900 g of olivine with an average particle size of 260 μm was used as
 150 bed material, having an experimental minimum fluidization velocity of 0.044 m/s. A constant
 151 flowrate of 0.3 kg/h of pellets was fed to the gasifier during the experiments. Steam preheated
 152 to 400 °C was used as fluidization media. The flowrate of steam fed to the gasifier was measured
 153 by an orifice plate and regulated with a needle valve to obtain a constant flowrate of 0.28 kg/h.
 154 This corresponds to a steam equivalence ratio of 4, defined as the ratio of the steam fed (0.93
 155 kg_{H2O}/kg_{biomass}) to that for stoichiometric conversion of the fuel into H₂ and CO (0.233
 156 kg_{H2O}/kg_{biomass} for a representative fuel composition of CH_{1.44}O_{0.66}) and it is comparable to the
 157 oxygen equivalence ratio used for combustion [33]. The fluidization velocity was 0.05 m/s

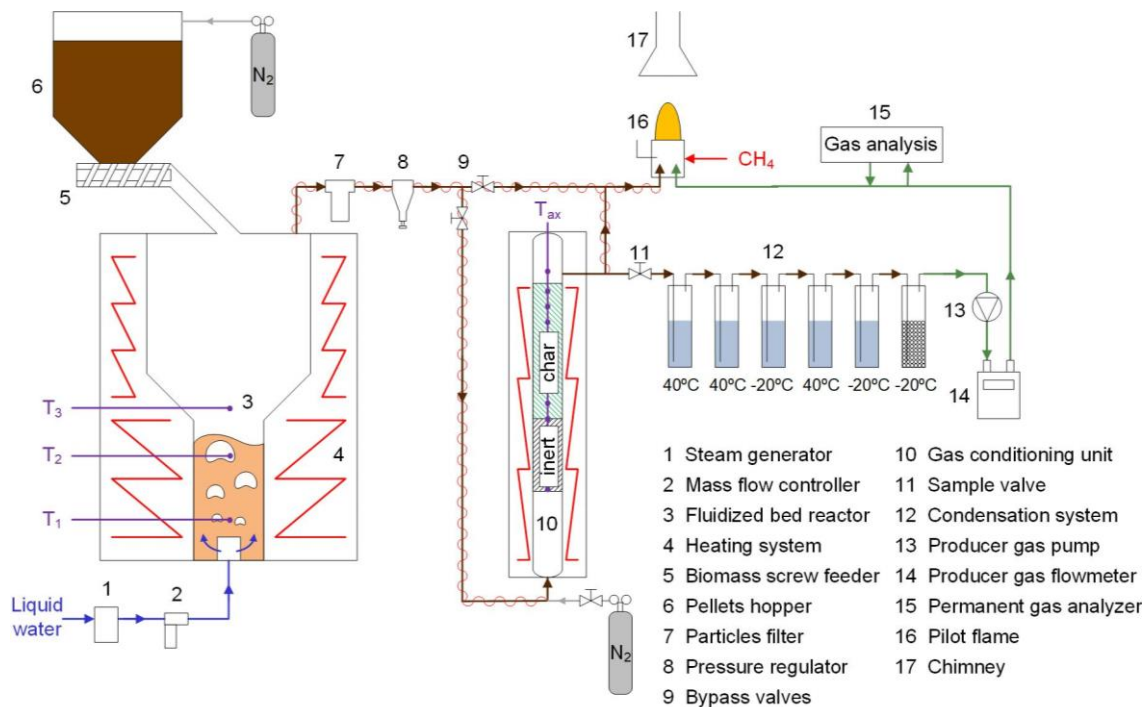
158 (slightly above that of minimum fluidization). The amount of feedstock supplied was controlled
 159 by a screw discharging on the bubbling bed. The feedstock tank was rinsed with 0.15 kg/h of
 160 nitrogen. The whole system including bed and feedstock tank was pressurized to an absolute
 161 pressure of 1.5 bar. Table 2 presents the average syngas composition produced in the gasifier.
 162 Due to small fluctuations in the conditions of the FB gasifier slight differences (below $\pm 2\%$) in
 163 the composition of the different syngas compounds were measured.

Compound	Concentration
H ₂ (% _v dry syngas)	35.1 ± 0.4
CO (% _v dry syngas)	17.7 ± 0.2
CO ₂ (% _v dry syngas)	16.9 ± 0.1
CH ₄ (% _v dry syngas)	6.3 ± 0.1
N ₂ (% _v dry syngas)*	24.1 ± 0.2
H ₂ O (% _v wet syngas)	49.7
GC-tar (g/Nm ³ dry syngas)	14

164 *by difference.

165 Table 2: Average syngas composition produced in the FB gasifier

166 The syngas was filtered in a sinter metal candle where particulate matter was removed. The
 167 filter and all gas lines were electrically heated to a temperature of 350 °C to prevent
 168 condensation of the tars. The gas flow after the filter can either be adjusted to go directly to a
 169 flare or through the secondary reactor, as shown in Fig. 2.



170
 171 Figure 2: Flowchart of the experimental set-up

172 2.2.2- Secondary char bed reactor

173 A FB configuration was selected for the secondary reactor. This configuration brings benefits
 174 over fixed/moving beds. On the one hand, fluidized beds prevent the appearance of high
 175 temperature gradients typically occurring in fixed beds, that may provoke rapid deactivation
 176 (due to low temperatures) or sintering phenomena (due to high temperatures) of the char. In

177 addition, fixed beds might clog during operation with dusty gas, such as the syngas produced in
178 fluidized bed gasifiers, due to the blocking of the bed pores by the fine particles carried by the
179 gas. However fluidized beds also present disadvantages compared to fixed/moving beds as the
180 poor contact between gas–char contact due to the bypass of gas through the bubbles.

181 The FB tar conversion unit used in this work consists of an electrically heated cylindrical tube
182 with an inner diameter of 37.2 mm. The syngas enters the reactor at the bottom at a
183 temperature of 350 °C and flows through a fixed bed of inert ceramic beads of 15 cm height to
184 preheat the gas to the target temperature in the reactor. An initial char bed of 32 g (discounting
185 the initial elutriation of fines), corresponding to a fixed bed height of 16 cm, was located on top
186 of the ceramic beads. The char used had an approximately disk like shape with a mean diameter
187 of 3.6 mm and a mean height of about 1 mm. The minimum fluidization velocity of the char was
188 measured to be approximately 0.48 m/s. The temperature inside the char bed was measured at
189 4 heights (5, 10, 15 and 20 cm above the bed of inert ceramic beads) in the center of the reactor
190 and, during operation, the temperature in the bed was uniform and remained constant,
191 indicating a proper mixing of the char particles.

192 During the experiments the spatial velocity was $24 \text{ Nm}^3_{\text{wet syngas}}/\text{kg}_{\text{char}}\text{h}$ while the superficial gas
193 velocity (volumetric gas flowrate divided by the open cross section of the reactor) in the
194 secondary reactor was between 0.75 m/s and 0.84 m/s, about 1.56 - 1.75 times the minimum
195 fluidization velocity of the char. The residence time of the syngas (τ) in the char bed was
196 calculated dividing the volume occupied by the char bed (considering it as a fixed bed with a
197 total weight of char of 32 g) by the flowrate of syngas produced in the FB gasifier; τ between
198 0.18 s and 0.2 s were obtained.

199 2.3- Operation procedure

200 Before each test the gasifier was operated for 3 h, bypassing the syngas directly to the flare, in
201 order to ensure constant regime of operation. Within the 3 h of stabilization, the secondary
202 reactor was filled with fresh char and heated to the desired temperature. During the heat-up of
203 the secondary reactor, a constant N_2 flow of 10 NI/min was set to ensure an inert atmosphere
204 preventing combustion of the char. As the target temperature in the reactor was reached, the
205 N_2 flow was stopped and the syngas produced in the FB gasifier was led through the secondary
206 reactor. It took about 30-45 minutes until the heating of the reactor adapted to the new flow
207 conditions and the char temperature reached a constant value. Once the desired temperature
208 was reached in the char bed, several tar samples were taken following the procedure described
209 in the tar protocol [34] using isopropanol as solvent. The tar-free syngas exiting the tar sampling
210 train was analyzed in a gas analyzer in order to quantify the concentration of the main
211 permanent gases.

212 Table 3 presents the target temperature in the secondary reactor and the time of tar samplings
213 taken in the seven tests performed. After the test, the char in the reactor was cooled down with
214 N_2 until its temperature was below 100 °C. The used char was collected and stored for further
215 analysis. It should be noted that during some of the tar samplings the temperature in the
216 secondary reactor did not reach the target temperature. These tar samples are noted in Table 3
217 as not valid and therefore not considered for presenting results of tar conversion.

218 Table 3: Target temperature in the secondary reactor and tar samplings taken during the
219 experiments with char bed

Test	Target temperature	Tar sampling 1	Tar sampling 2	Tar sampling 3	Tar sampling 4	End test
(-)	(°C)	(hh:mm)	(hh:mm)	(hh:mm)	(hh:mm)	(hh:mm)
1	850	00:39 (not valid, low T)	01:49	-	-	2:39
2	850	00:55	02:35	04:15	-	4:35
3	850	00:45 (not valid, low T)	-	-	-	1:00
4	850	00:20 (not valid, low T)	01:50	3:20	-	3:35
5	750	00:35	01:44	03:04 (not valid, low T)	-	3:49
6	850	00:45	01:45	04:15	06:15	6:30
7	875	01:16	02:06	03:26	04:56	5:11

220

221 2.4- Experimental conditions

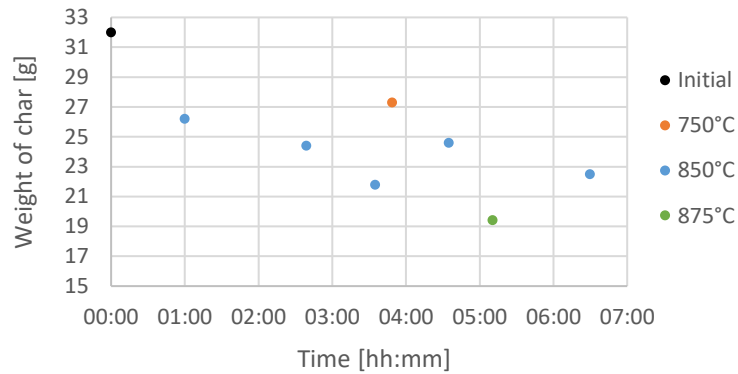
222 2.4.1- Experimental conditions in the FB gasifier

223 The FB gasifier producing the syngas necessary for the tests operated at 750 ± 5 °C and $1.5 \pm$
224 0.01 bar. Due to the low operation temperature, the char produced during the fuel
225 devolatilization stage was not completely converted. Consequently, char accumulated in the
226 dense bed of the gasifier during the tests. The FB gasifier was opened to remove the char
227 accumulated only two times during the whole campaign being the amount recovered 58 g
228 (removed after Test 4, see Table 3) and 31 g (removed after Test 7) respectively. Olivine and
229 char particles were separated by sieving since the latter were significantly larger. Considering
230 the total amount of olivine in the reactor, 900 g, char accumulation in the bed is not considered
231 to significantly influence the fluidization quality, which was assumed to be governed by the
232 olivine particles.

233

234 2.4.2- Experimental conditions in the secondary reactor

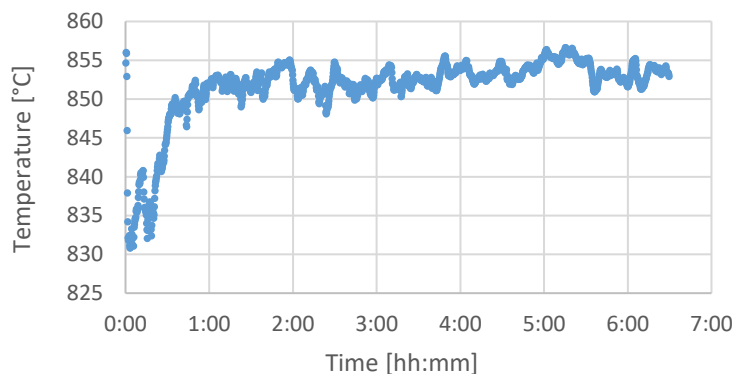
235 As explained before the secondary reactor was loaded before each test with 32 g of char. The
236 amount of char remaining in the secondary reactor at the end of each test was below 32 g for
237 all the conditions tested (see Fig. 3). Blue dots represent the char remaining in the char bed after
238 the five experiments at 850 °C while the orange and green dots represent the char remaining
239 after the experiments at 750 °C and 875 °C, respectively. The black dot represents the initial
240 amount of char in the bed. The reduction in the amount of char in the bed could indicate a net
241 C consumption during the experiments. However, some attrition/elutriation phenomena may
242 have occurred resulting in some losses of char. Although elutriation loss is expected to be a
243 minor amount compared to the initial char load, it was not systematically investigated.
244 Therefore, this uncertainty prevents establishing a clear boundary temperature dividing positive
245 and negative C balance conditions.



246

247 Figure 3: Char bed weight after the tests. Orange dot: test at 750 °C; Blue dots: tests at 850 °C;
 248 Green dot: test at 875 °C.

249 Fig. 4 displays the temperature profile during one test at 850 °C. When the syngas is driven into
 250 the preheated secondary reactor the temperature of the char bed decreases rapidly (till about
 251 830 °C in Figure 4) due to the lower temperature (350 °C) of the piping connecting the FB gasifier
 252 and the secondary reactor. It is necessary between 30 and 45 min to reach the target
 253 temperature again. This lower temperature at the beginning is the reason why the first sampling
 254 of tests number 1, 3 and 4 conducted at 850°C were considered as not valid. Once the
 255 temperature was reached, very slight fluctuations, ± 5 °C were observed. During operation, the
 256 temperature at the four different heights in the char bed remains almost equal and constant
 257 with time, indicating a proper mixing of the char particles in the bed.



258

259 Figure 4: Evolution of the mean temperature of the char bed during the test number 6 at 850
 260 °C

261 2.5- Analysis

262 2.5.1- Gas and tar analysis

263 During tar samplings a tar-free syngas stream was led to an ABB AO2020 gas analyzer, where
 264 concentration of the permanent gases CO, CO₂, CH₄, O₂ and H₂ were measured. The amount of
 265 N₂ was calculated by difference. Tar samples were analyzed by GC-FID using a Shimadzu GC 2010
 266 equipped with an Agilent 19091S-433 capillary column. The concentration of 25 compounds
 267 from benzene to perylene were given. Analytical standards of each quantified compound were
 268 used for calibration during the analytical protocol. However, due to some analytical problems,
 269 the concentration of phenol and cresols were not properly determined. Therefore, the
 270 information concerning tar class 2 (TC2) compounds (heteroatomic aromatic tars) are not given.
 271 The different tar compounds were lumped according with the classification described in [35]

272 being TC3 monoaromatic tars (without O or N on its composition), TC4 aromatic compounds
273 with 2-3 aromatic rings and TC5 aromatic compounds with 4-7 aromatic rings.

274 2.5.2- Char analysis

275 The CHNS content of the spent char samples was determined in an elemental analyzer
276 (Elementar Vario EL-III) and the content of inorganic species was measured with an ICP-OES
277 (Varian 720-ES) after digestion in a microwave with H₂O₂ and HNO₃.

278 To characterize the surface physical structure of the chars, i.e. specific surface area, pore
279 volume, and pore size distribution, N₂ adsorption measurements were performed. The
280 adsorption/desorption isotherms were measured in an Autosorb MP-1 (Quantachrome
281 Instruments) in the relative pressure range of $\sim 2 \times 10^{-5}$ – 0.99. The BET (Brunauer-Emmett-
282 Teller) model was applied to determine the total specific surface area. The total volume was
283 determined at a relative pressure close to 1, assuming that in these conditions all N₂ in the pores
284 is in liquid state. Micropore and mesopore specific surface area and volume were determined
285 with the QSDFT model (Quenched Solid Density Functional Theory) applied to the adsorption
286 branch, considering slit/cylindrical pores. The conditioning of the char samples previous to the
287 adsorption measurements included drying at 106 °C for 90 minutes, followed by milling and
288 degassing in vacuum at 150 °C for 8 hours to remove species adsorbed on the char surface.

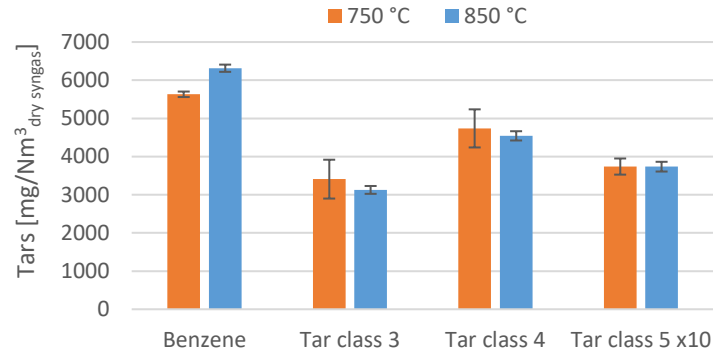
289 SEM-EDX analysis was performed to examine morphology, structure variation and surface
290 composition of the spent char samples. The SEM-EDX analyses of the different chars were
291 carried out by means of FEGSEM (Field Emission Gun Scanning Electron Microscopy) FEI Teneo™.

292

293 **3- Results and discussion**

294 3.1- Tar evolution

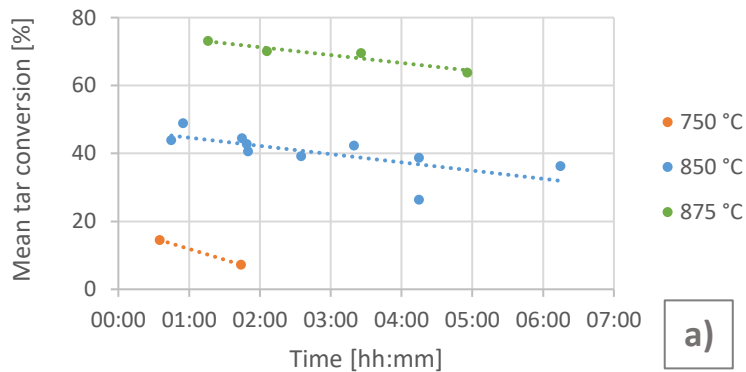
295 Preliminary experiments were conducted to measure the composition in the raw gas and to
296 estimate the possible extent of thermal tar cracking in the secondary reactor without char. This
297 was done in order to obtain a reference concentration of tar to which the extent of
298 heterogeneous catalytic conversion over char can be referred. Fig. 5 presents the composition
299 of the tar mixture of the raw gas and after thermal cracking in the secondary reactor preheated
300 at 850 °C without char but with the pre-bed of ceramic beads loaded. The results presented for
301 the raw gas are the average of three tests taken at the beginning, in the middle and at the end
302 of the seven tests presented in Table 3. The tar results for the thermal cracking at 850 °C are the
303 average of two samples taken in one day of operation. The obtained standard deviations are
304 very low for each case (see Fig. 5), which shows the stability of the producer gas composition
305 (during the campaign). The thermal tar cracking tests at 850 °C led to a slight increase in the
306 concentration of benzene compared to the raw gas, from 5600 mg/Nm³ to 6300 mg/Nm³, while
307 the reduction over the concentration of tar classes 3, 4 and 5 in the syngas was almost negligible.
308 Therefore, the influence of thermal tar cracking at this temperature is minor. The composition
309 of the tar mixture in these tests were used to calculate the tar conversion in the experiences
310 with char at 750 °C (raw gas) and at 850/875 °C (thermal tar cracking at 850 °C).



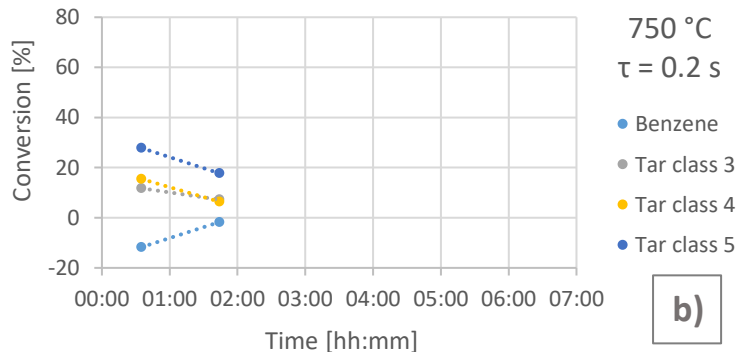
311

312 Figure 5: Yields of the different tar classes of the raw gas (750 °C) and with the secondary
 313 reactor at 850 °C in absence of char bed

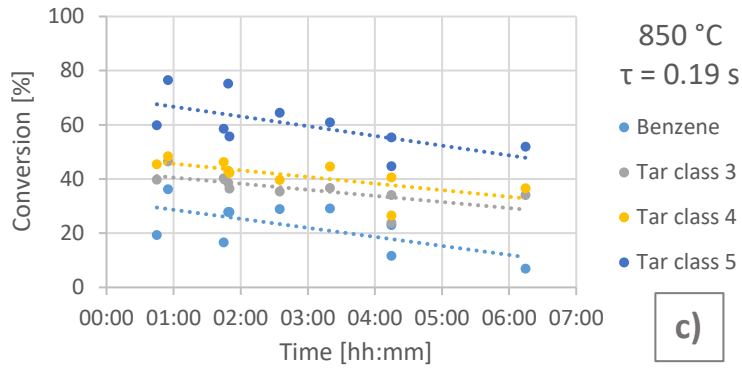
314 Fig. 6 shows the evolution of tar conversion obtained for the different tar classes over the char
 315 bed at the three temperatures tested in the secondary reactor. In Fig. 6a the evolution of the
 316 average tar conversion (excluding benzene) at the three temperatures tested is presented.
 317 According to the results, the char bed temperature has an important impact on the average tar
 318 conversion. After 1-2 hours of operation the mean tar conversion at 750 °C was around 10 %
 319 while at 850 °C and 875 °C the tar conversion increased up to 45 % and 70 % respectively. This
 320 is probably due to the enhancement in the steam gasification rate of char/soot, promoting the
 321 presence of active sites onto the char surface with increasing temperature. The increase in the
 322 tar conversion as temperature was raised from 850 °C to 875 °C is especially remarkable.



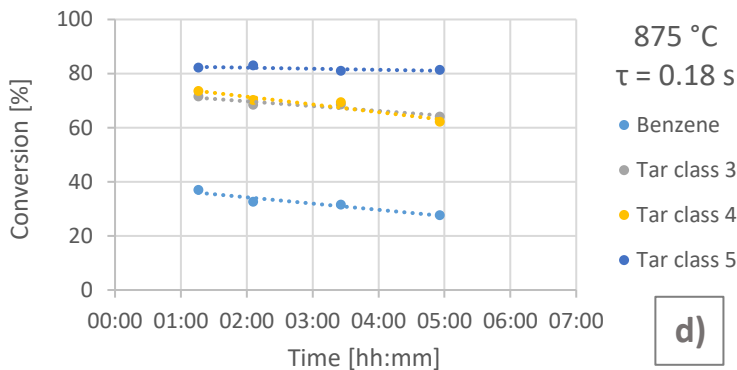
323



324



325



326

327 Figure 6: Evolution of the tar conversion during the experiments. 6a: Evolution of the mean tar
 328 conversion (excluding benzene) at different temperatures. 6b, 6c, 6d: Evolution of the
 329 conversion of the different tar classes at 750, 850 and 875 °C, respectively.

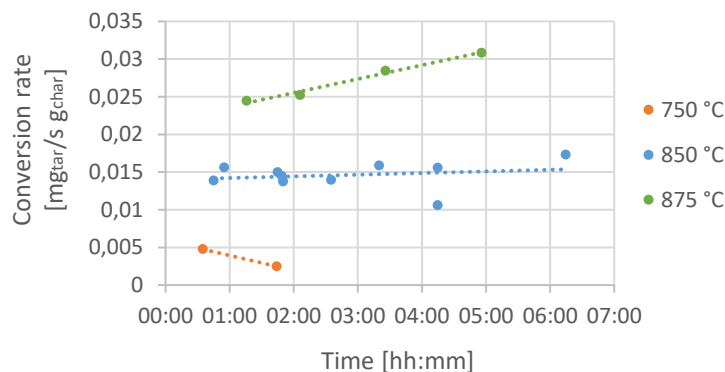
330 At 750 °C (Fig. 6b) the conversion of the different tar classes was rather low, even at the
 331 beginning of the test. Only 28 % of the heaviest tars (TC5) were converted using a char bed after
 332 35 min of operation. The conversion of these heavy tars further decreased to below 18 % one
 333 hour later. The trend measured for lighter tars was similar but the conversions are slightly lower
 334 since, as expected, heavier tar molecules are converted faster over char than lighter tars. In the
 335 two tar samples taken at 750 °C the conversion of benzene was negative indicating a slight
 336 increase in the benzene concentration with respect to the reference test without char. This
 337 result, in agreement with previous work [32], could be explained by the enhancement of
 338 cleavage of alkyl and polyaromatic tars into smaller compounds, such as benzene, over the
 339 surface of the char.

340 Fig. 6c presents the conversion of the different tar classes obtained in the five tests, of different
 341 duration, performed at 850 °C. The dispersion of the experimental results is, most likely, the
 342 consequence of small differences in the gasifier conditions during the different days of
 343 operation. When the secondary reactor temperature was increased from 750 °C to 850 °C the
 344 conversion of the different tar classes over char was significantly enhanced. After 45 min of
 345 exposure of the char bed to the syngas-tar mixture the conversion of TC5 was around 70 %,
 346 while for TC4 and TC3 the conversions were between 40 and 50 %. Benzene was, as expected,
 347 the compound with the lowest conversion over the char bed. With increasing time of exposure
 348 of the char bed to the syngas-tar mixture, a reduction in tar conversion was observed for every
 349 tar class. This reduction was, after 6 h of test, around 30 % for TC3, TC4 and TC5 as compared
 350 with the initial conversion (i.e., the conversion of TC3 was reduced from around 70% to 50%).
 351 For benzene the conversion decrease was even larger. This reduction in the conversion of the

352 different tar classes could be explained by the 30 % of reduction in the weight of char in the bed
353 after 6 h of experiment since the activity of the char, defined as the ratio between the tar
354 conversion rate at time t and the initial tar conversion rate at each temperature, was stable
355 during the operation at 850 °C (see Fig. 7).

356 Increasing the char temperature to 875 °C (Fig. 6d) led to a further enhancement of the initial
357 tar conversion for the different tar classes. After 75 min of test the conversion of TC5 was above
358 80 % with a syngas residence time in the char bed of 0.18 s. The conversions of TC3 and TC4
359 were above 70 % while the reduction in the concentration of benzene was between 30 and 40
360 %. The most important difference with the results obtained at 850 °C was the evolution
361 conversion along the time for the different tar classes. While the conversion of TC5 kept
362 practically constant at 875 °C after 5 h of test, it was significantly reduced with time at 850 °C.
363 For the other tar classes, the decay in the conversions measured was much lower at 875 °C than
364 at 850 °C. These observations suggest that an adequate selection of the experimental conditions
365 in the secondary char reactor could provide high conversion of heavy tars for long operation
366 times. This is especially relevant since heavy polyaromatic tars are the compounds of the syngas
367 responsible for the high tar dew point and its end-use related problems.

368 In order to analyze the catalytic activity of the char during the experiments, the tar conversion
369 rate (excluding benzene) was calculated based on experimental results. Fig. 7 presents the
370 evolution with time of the tar conversion rate, in milligrams of tar converted per second and
371 gram of char remaining in the bed, for the three temperatures studied. Since the experimental
372 data of the amount of char remaining in the bed at the different temperatures tested is
373 insufficient to model the char conversion process, a linear char consumption was assumed for
374 the calculations. This simplification does not provide a detailed evolution of char consumption,
375 but it allows to track the evolution of tar conversion rate trend (increase/decrease). At 750 °C
376 the tar conversion rate was rather low, even at the beginning of the experiment. At 850 °C the
377 char activity was clearly higher and the measured catalytic conversion rate of tars seemed to
378 reach a plateau at values around 0.015 $\text{mg}_{\text{tar}}/(\text{s}\cdot\text{g}_{\text{char}})$. However, at 875 °C the tar conversion rate
379 per gram of char seemed to rise slightly from 0.024 to 0.031 $\text{mg}_{\text{tar}}/(\text{s}\cdot\text{g}_{\text{char}})$ during the experiment.
380 After 5 h of test at 875 °C the char bed with an initial weight of 32 g had converted approximately
381 12 g of tars (benzene not included) and the catalytic activity of the material was slightly higher
382 than the initial one (at the beginning of the test). This result highlights the capability of non-
383 preactivated biomass chars to be used as catalysts for tar abatement in reactor systems where
384 the experimental conditions can be controlled to avoid rapid deactivation. A tar conversion
385 device aiming at operating in continuous would provide, in the conditions analyzed, a high tar
386 conversion rate and a low catalyst (char) consumption.



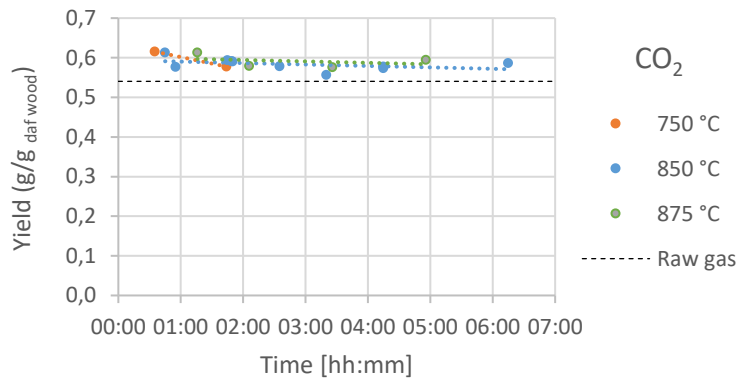
387

388

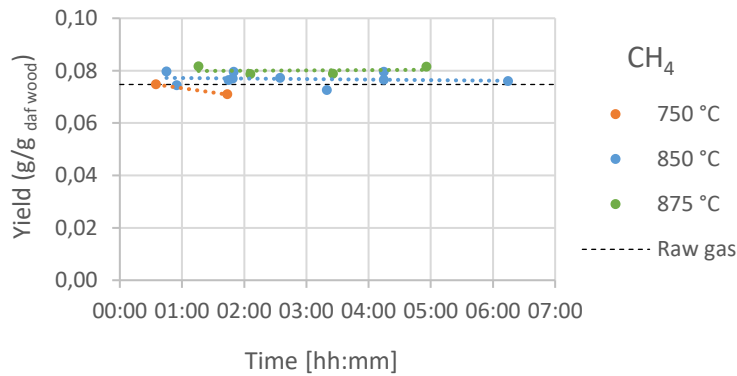
Figure 7: Evolution of the tar conversion rate at different temperatures.

389 3.2- Permanent gases evolution

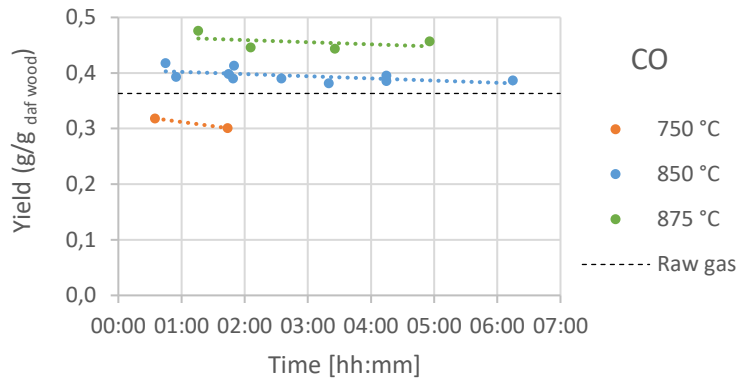
390 Fig. 8 shows the yields of the main gaseous species in the syngas after the secondary char bed
391 at the three temperatures studied, as well as those in the raw gas for reference. CO and H₂ are
392 clearly influenced by the char bed temperature and by the duration of the test. The gasification
393 rate of char increases at higher temperatures, which explains the higher CO and H₂ yields
394 obtained at higher temperatures. The reduction in CO and H₂ yields with time can be explained
395 by the progressive consumption of the char bed during the tests. In contrast, the yield of CO₂ in
396 the syngas increase slightly after the char bed, but it is hardly affected by the temperature in the
397 secondary reactor, nor by the duration of the test, likely due to the consequence of the
398 enhancement of the water gas shift reaction provoked by the presence of catalytic elements in
399 the char. The yield of CH₄ shown in Fig. 8b is slightly influenced by the char bed temperature
400 indicating a net production of this compound in the secondary reactor, probably as a result of
401 the enhancement with temperature of conversion of alkyl-aromatic species over char, such as
402 toluene [12]. The thermal conversion of volatiles in the secondary reactor could be also partially
403 responsible of the increase in CH₄ yield [36].



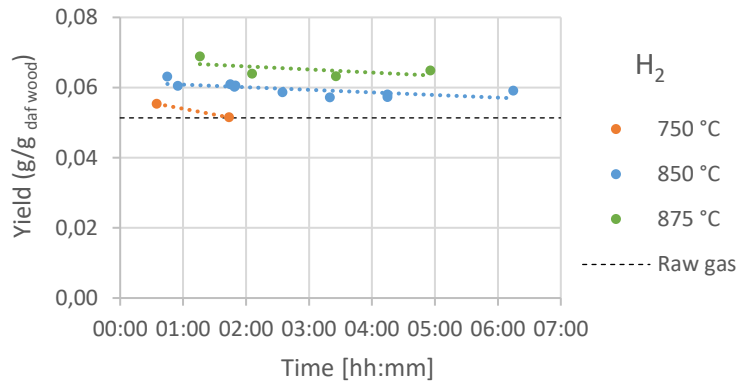
404



405



406



407

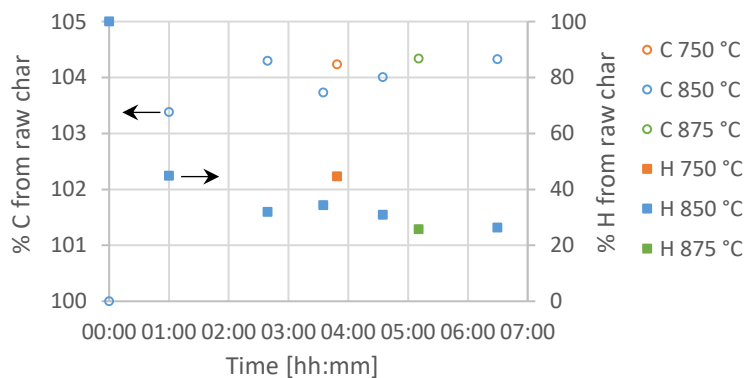
408 Figure 8: Evolution of the yield of the main permanent gases at different temperatures.
 409 Horizontal black dotted lines represent the corresponding yield of the species in the raw
 410 syngas

411

412 3.3- Char characterization

413 3.3.1 – Elemental composition

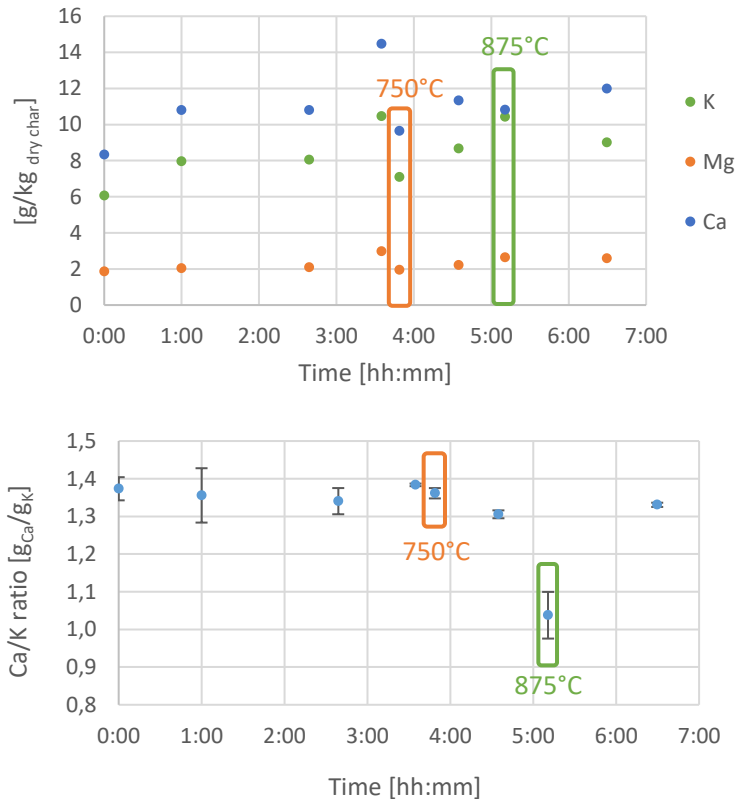
414 Fig. 9 shows the evolution of the carbon and hydrogen content of the spent char after each
 415 experiment in relation to the contents in the original raw char. It can be seen that there is a
 416 tendency of increase in the carbon content and decrease in the hydrogen content along time for
 417 the experiments at 850 °C, especially during the first hour of the experiment. In the case of
 418 hydrogen, this tendency is enhanced at 875 °C and reduced at 750 °C. These tendencies may be
 419 due to cleavages of functional groups with hydrogen and oxygen in the char structure, which are
 420 enhanced at the beginning of the test because the char was produced at a lower temperature
 421 (700 °C) than those in the experiments.



422

423 Figure 9: Carbon and hydrogen content of spent char (as a percentage of C and H content in
424 raw char) along the time of the test at the three temperatures.

425 Figure 10 presents the analysis by ICP of the main inorganic elements in the char samples. A
426 slight tendency of increase in the concentration of inorganic elements during conversion can be
427 observed. This is probably due to char gasification, which decreases the content of organic
428 elements while increasing the content of inorganics. According to the results, no major release
429 of the main alkali and alkali earth metals (K, Mg and Ca) was measured and, in spite of the higher
430 volatility of alkali metals compared to that of alkaline-earth metals [37], the Ca/K ratio decreased
431 when the temperature is raised to 875 °C.



432

433

434 Figure 10: Content of main inorganic elements (top) and Ca/K mass ratio (bottom) in spent
435 char. The values of the experiment at 750 °C are inside an orange box and at 875 °C inside a
436 green box; other experiments were conducted at 850 °C.

437

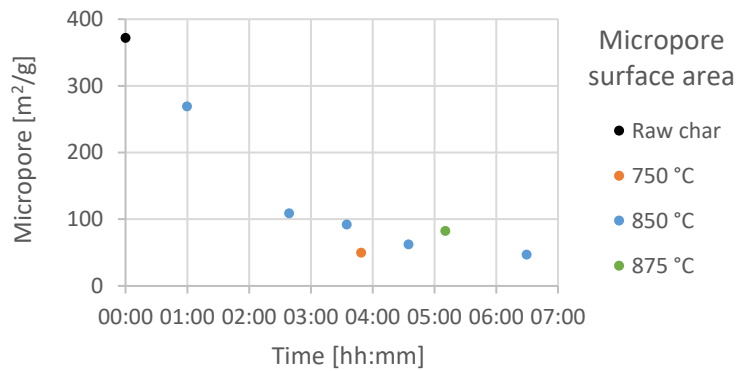
438 3.3.2 – Surface area and pore volume

439 During the exposure to the tar loaded syngas, the char bed undergoes structural changes
440 modifying its characteristics as a catalyst. Fig. 11 presents the evolution of the internal structure
441 (surface area and pore volume) of the char during the tests. The original char (raw char) is
442 characterized by a rather large total specific surface area (SSA), originated mainly by micropores.
443 This behavior is typical of char produced from woody biomass at temperatures above 600 °C in
444 a N₂ atmosphere [38]. Analyzing the evolution of the char structure at 850 °C within the first two
445 hours, a significant reduction in both micropore surface area and micropore volume can be
446 observed, accompanied by an increase in mesoporosity. Consequently, after two hours of test,
447 most of the total pore volume and above 50 % of the total surface area correspond to
448 mesopores. This initial evolution of the char internal structure may be the consequence of the

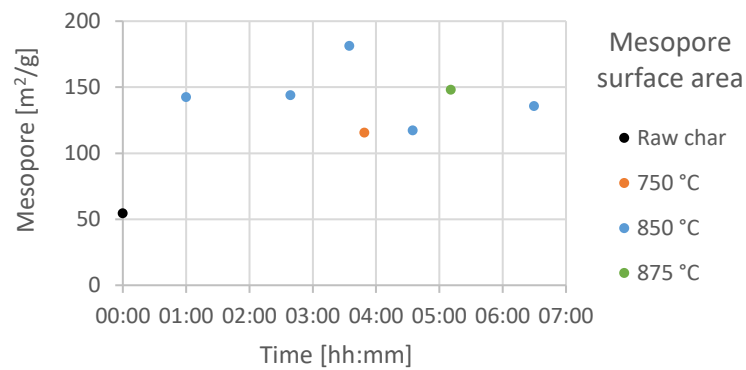
449 collapse, due to the rapid initial char gasification, of the walls separating the original micropores.
 450 At longer residence times the amount of micropores in the char continued decaying to below
 451 $0.025 \text{ m}^3/\text{g}$ and $50 \text{ m}^2/\text{g}$ while the amount of mesopores stabilized around $0.2\text{-}0.25 \text{ m}^3/\text{g}$ and
 452 $140 \text{ m}^2/\text{g}$. Since the volume of mesopores did not increase after the first two hours, the
 453 reduction in the amount of micropores must be the consequence of the pore mouth blocking
 454 mechanism [18] produced by the deposition and coking of tars on the pore entrance.

455 During the test at $850 \text{ }^\circ\text{C}$ the activity of the char decayed around 15-20 % (see Fig. 7). However,
 456 after the initial rapid modification of the char structure, the reduction in the micropore area was
 457 above 80 % while the mesopore area remained almost constant. These observations let us to
 458 conclude that, during the tests, the tar conversion process is taking place mainly in the
 459 mesopores of the char. In a recent work a linear correlation between the total mesopore area
 460 available in the char bed and the tar conversion rate constant were found [19], highlighting the
 461 significance of mesopores for tar conversion. As mentioned in the Introduction, diffusional
 462 limitation could inhibit the conversion of tar compounds inside narrow micropores.

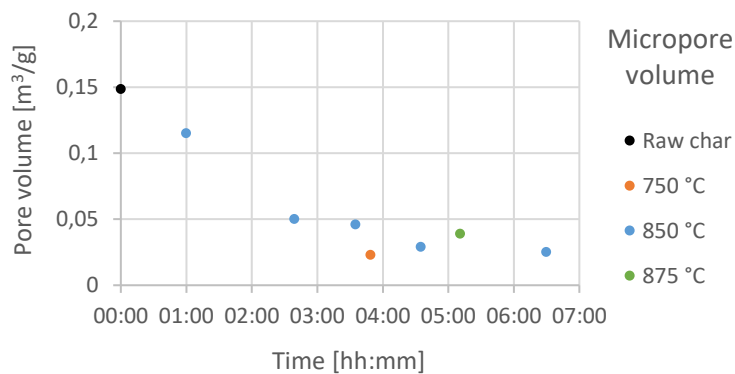
463

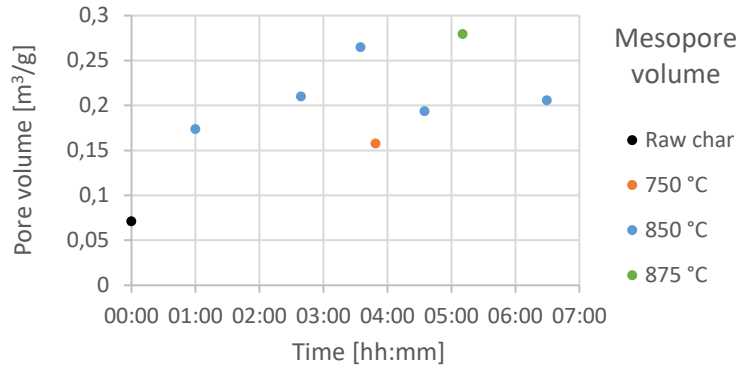


464



465





466

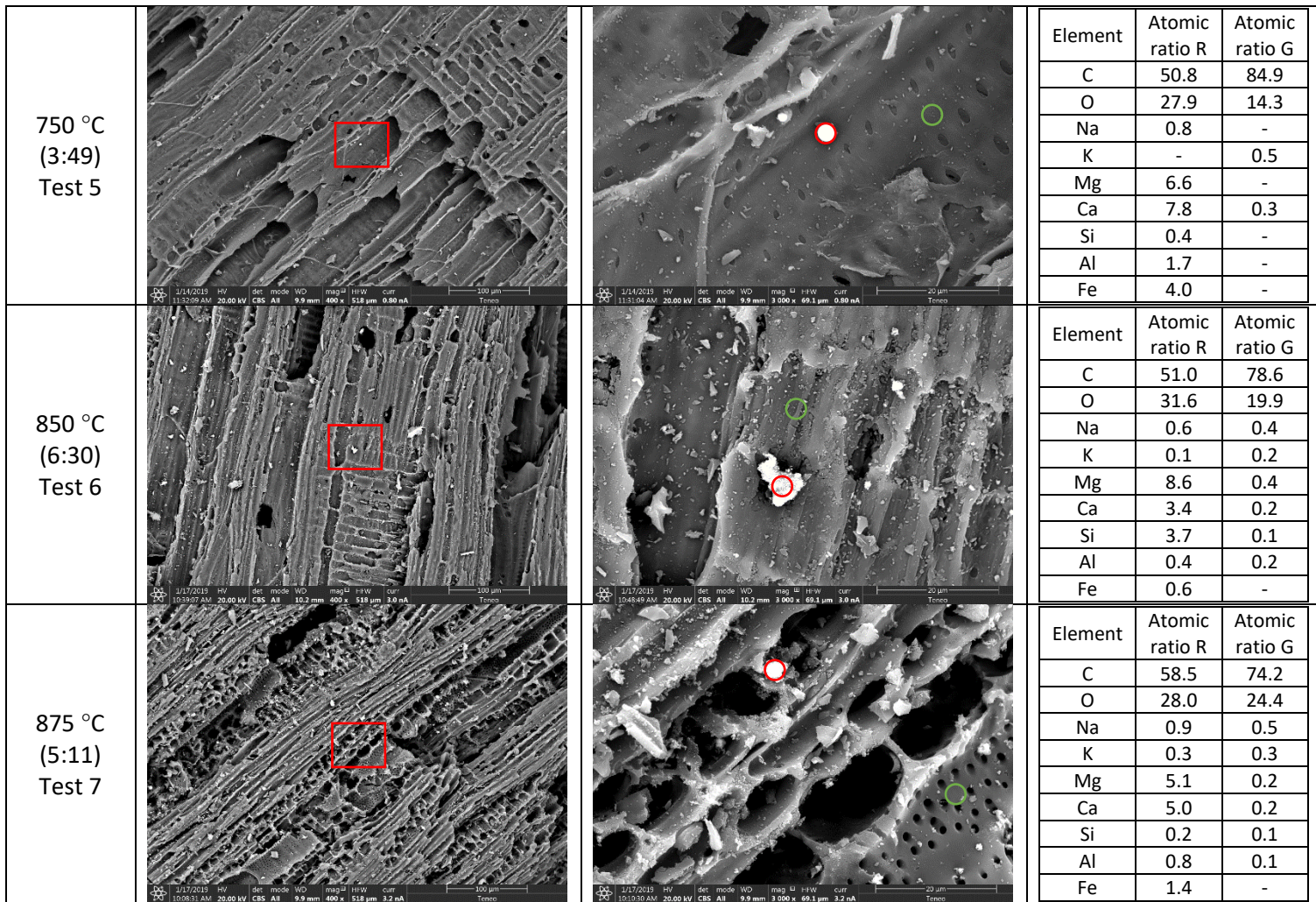
467 Figure 11: Evolution with time of the micropore and mesopore surface areas and volumes at
 468 the different temperature.

469

470 3.3.3 – SEM-EDX analysis

471 Fig 12 presents the results of the SEM-EDX analysis made on four different char samples; the
 472 original “raw” char, the char after 3 h and 49 min of exposure to the syngas at 750 °C (Test 5 in
 473 Table 3), the char after 6 h and 30 min of exposure to the syngas at 850 °C (Test 6) and the char
 474 after 5 h and 11 min of exposure to the syngas at 875 °C (Test 7). Two pictures at different
 475 magnifications are presented to show a general perspective of the char surface (400x
 476 magnification) and a closer image where the presence of inorganic clusters can be visualized and
 477 analyzed by EDX (3000x magnification). The red squares presented over the 400x magnification
 478 pictures represent the area magnified at 3000x on the picture of the right. The red and the green
 479 circles on the image at 3000x of magnification indicate the area where the EDX analysis were
 480 made. The atomic ratios of the white clusters dispersed on the char surface (red circles) and the
 481 atomic ratios of the dark carbonaceous surface (green circles) obtained by EDX are presented
 482 on the right tables.

Sample (time of exposure)	Magnification 400x	Magnification 3000x	EDX analysis		
			Element	Atomic ratio R	Atomic ratio G
Raw char			C	29.0	85.0
			O	33.0	13.7
			Na	1.3	0.1
			K	0.1	0.5
			Mg	9.3	0.4
			Ca	13.1	0.2
			Si	6.4	0.1
			Al	3.9	0.1
			Fe	3.9	-



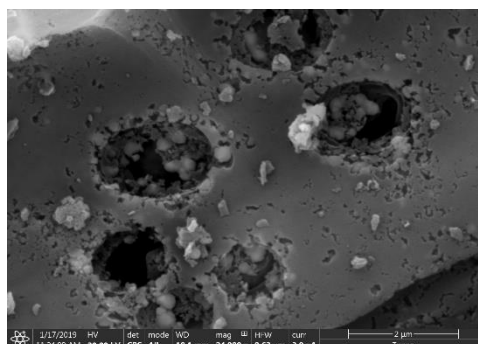
483

484 Figure 12: SEM images and EDX analysis of char samples produced at different temperatures.

485 SEM images at 3000x are the area confined in red squares in the SEM images at 400x. EDX
486 analysis R and G represent the elemental analysis in the area confined by red and green circles
487 in the SEM images at 3000x.

488 All the samples analyzed, regardless the severity of the conversion process, present the
489 characteristic fibrous structure of wood-derived chars. However, at the highest temperature
490 tested (875 °C), several pores not present at lower temperatures can be observed. In Fig. 13, an
491 image at 24000x of magnification over the surface of the char after exposure to the syngas at
492 875 °C reveals the ongoing consumption of the char matrix and the formation of new pores (the
493 smallest pores in the picture fall within the size range of mesopores).

494



495 Figure 13: SEM image at 24000x of the spent char after 5 h and 11 min of exposure to the
496 syngas at 875 °C.

497 In agreement with previous study [19], two different phases can be visually distinguished: a dark
498 continuous phase and clusters of a white phase onto the dark surface. According to the images
499 presented in Fig. 12 the proportion of white clusters is much lower in the raw char and the spent
500 char at 750 °C than for spent chars at 850 °C and 875 °C. Additionally, a significant difference
501 can be observed in the shape of these clusters. In the two first images (raw char and the spent
502 char at 750 °C) the clusters are apparently round-shaped while in the chars of the two last
503 images the clusters adopt an irregular structure. According to the EDX analysis presented, these
504 white clusters are characterized by a low atomic proportion of C and a high proportion of
505 alkaline-earth metals (Mg and Ca). On the other hand, the dark phase is mostly composed of C
506 and O with traces of other elements. It is important to highlight that, in spite of the different
507 proportion found for alkaline-earth metals, alkali metals present similar atomic proportions in
508 both phases. Therefore, while magnesium and calcium tend to segregate during the conversion
509 process into a different phase (white clusters), potassium, a well-known catalytic element,
510 seems to present larger atomic proportions in the dark phase (char matrix).

511 The absence of white clusters in the char sample obtained at 750 °C is, most likely, the
512 consequence of the higher tar deposition rate compared to the char/soot gasification rate. In
513 these conditions the tar adsorbed onto the active sites of the char surface undergoes
514 polymerization creating soot deposits, reducing the char porosity and hindering the interaction
515 of active sites with gaseous tar. At 875 °C the temperature is high enough to gasify soot at a
516 higher rate than the deposition rate. During gasification of the char matrix, the volatile alkali
517 metals are released to the gas stream while the less volatile alkaline-earth metals tend to
518 accumulate in the observed white clusters. However, white clusters are most likely released to
519 the gas phase during the char conversion since, according to ICP analysis, the Ca/K ratio does
520 not significantly vary during the tests at 850 °C, whereas it decreases as reactor temperature is
521 raised to 875 °C.

522 According to this, the presence of a high concentration of white clusters can indicate high activity
523 of the char. However, even if the presence of AAEM elements is straightforwardly related with
524 the char activity [19], the influence of white clusters on tar conversion process is not clear yet.
525 White clusters may be directly involved in tar catalytic conversion or maybe it is the dark phase
526 (char matrix) that, in high gasification rate conditions, provides the active sites necessary for a
527 high tar conversion rate. Future experiments will be targeted to analyze these options.

528

529 **4- Conclusions**

530 The present work analyzes the catalytic conversion of the tars present in a real syngas, produced
531 in a steam-blown FB gasifier, over a FB of non-activated wood-derived char. Temperatures
532 between 750 °C and 875 °C with spatial velocities of 24 Nm³/kg_{char}h corresponding to gas
533 residence time on the char bed between 0.18 s and 0.2 s were tested. The evolution of the tar
534 conversion in the bed, the gas species in the syngas and the internal structure of the used
535 catalysts were determined in order to analyze the viability of using this material for syngas
536 cleaning downstream char reactors.

537 The main conclusions are:

- 538 - A long-term test conducted at 875 °C during 5 hours resulted in tar conversions in the
539 range of 64 – 73 % along the test. The reduction in conversion with time was probably
540 due to char consumption (gasification) rather than deactivation.
- 541 - Long-term tests conducted at 850 °C showed initial tar conversions close to 50 %, with
542 a tendency of char deactivation along the test till around 35 % after 6 hours of service.
543 The test conducted at 750 °C showed much lower conversion (\approx 15 %) and a significant
544 deactivation after 2 hours.
- 545 - High tar conversion rates and increasing activities of the char can be achieved using non-
546 activated biomass chars given that the reactor conditions promote high enough carbon
547 consumption (from deposited soot) by gasification.
- 548 - The heaviest tars present in a real syngas mixture are converted faster than lighter tars
549 over a char catalyst, confirming literature results using syngas doped with tar
550 compounds.
- 551 - The results suggest that the tar conversion takes place mainly in the mesopores of the
552 char particles.
- 553 - The presence of a high concentration of white clusters over the char surface, containing
554 a significant proportion of alkaline-earth elements, are indicative of a high activity of the
555 char towards tar conversion.

556

557 **Acknowledgments**

558 The authors want to express their appreciation to and Mr. Israel Pardo Arias and Mr. Hernán
559 Almuiña Villar for their support and advice during SEM-EDX analysis and setting up the tar
560 cracking reactor, respectively. The authors gratefully acknowledge the financial support given by
561 European Union's Horizon 2020 Research and Innovation Programme under grant agreement
562 number 731101 (BRISK II) and by the Spanish Ministry of Economy and Competitiveness and the
563 European Union-FEDER in the project NETuWAS (CTM2016-78089-R).

564

565

566

- [1] A. Gómez-Barea, B. Leckner. Gasification of biomass and waste, in: M. Lackner, F. Winter, A.K. Agarwal (Eds.), *Handbook of Combustion*, vol. 4, Wiley-VCH, Weinheim, 2009, pp. 365–397.
- [2] C. Hignman, M. van der Burgt. *Gasification*, second ed. Gulf Professional Publishers/Elsevier Science, Amsterdam, 2008.
- [3] Gómez-Barea A, Leckner B, Villanueva Perales A, Nilsson S, Fuentes-Cano D. Improving the performance of fluidized bed biomass/waste gasifiers for distributed electricity: a new three-stage gasification system. *Appl Therm Eng* 50 (2013) 1453–1462.
- [4] D.J. Stevens. *Hot Gas Conditioning: Recent Progress with Larger-Scale Biomass Gasification Systems*, NREL, Golden, CO, USA, 2001, Report no. NREL/SR-510- 29952.
- [5] P. Hasler, T. Nussbaumer. Gas cleaning for IC engine applications from fixed bed biomass gasification, *Biomass Bioenergy* 16 (1999) 385–395.
- [6] H. Boerrigter, “OLGA” Tar Removal Technology, The Energy Research Centre of the Netherlands, 2005, ECN-C-05-009.
- [7] D. Sutton, B. Kelleher, J.R.H. Ross. Review of literature on catalysts for biomass gasification, *Fuel Process. Technol.* 73 (2001) 155–173.
- [8] P. Simell, *Catalytic Hot Gas Cleaning of Gasification Gas*, VTT Publication No 330 (1997).
- [9] Z. Abu El-Rub, E.A. Bramer, G. Brem, *Fuel* 87 (2008) 2243–2252
- [10] S. Hosokai, K. Kumabe, M. Ohshita, K. Norinaga, K. Matsuoka, C.Z. Li, J.I. Hayashi. Mechanism of decomposition of aromatics over charcoal and necessary condition for maintaining its activity, *Fuel* 87 (2008) 2914–2922.
- [11] P. Brandt, E. Larsen, U. Henriksen. High tar reduction in a two-stage gasifier, *Energy Fuels* 14 (2000) 816–819.
- [12] D.M.L. Griffiths, J.S.R. Mainhood. Cracking of tar vapor and aromatic compounds on activated carbon, *Fuel* 46 (1967) 167–176.
- [13] D. Fuentes-Cano, A. Gómez-Barea, S. Nilsson, P. Ollero. Decomposition kinetics of model tar compounds over chars with different internal structure to model hot tar removal in biomass gasification, *Chem. Eng. J.* (2013) 1223–1233.
- [14] G. Ravenni, Z. Sárosy, J. Ahrenfeldt, U.B. Henriksen. Activity of chars and activated carbons for removal and decomposition of tar model compounds – A review. *Renew Sust Energ Rev* 94 (2018) 1044–1056
- [15] T. Matsuhara, S. Hosokai, K. Norinaga, K. Matsuoka, C.Z. Li, J.I. Hayashi. In-situ reforming of tar from the rapid pyrolysis of a brown coal over char. *Energy Fuels* 24 (2010) 76–83.
- [16] U. Henriksen, J. Ahrenfeldt, T.K. Jensen, B. Gøbela, J.D. Bentzen, C. Hindsgaula, L.H. Sørensen. The design, construction and operation of a 75 kW two-stage gasifier. *Energy* 31 (2006) 1542–1553.
- [17] R.Ø. Gadsbøll, Z. Sarossy, L. Jørgensen, J. Ahrenfeldt, U.B. Henriksen. Oxygen-blown operation of the TwoStage Viking gasifier. *Energy* 158 (2018) 495–503.
- [18] R. Moliner, I. Suelves, M. Lazaro, O. Moreno. Thermocatalytic decomposition of methane over activated carbons: influence of textural properties and surface chemistry, *Int. J. Hydrog. Energy* 30 (2005) 293–300.
- [19] D. Fuentes-Cano, F. Parrillo, G. Ruoppolo, A. Gómez-Barea, U. Arena. The influence of the char internal structure and composition on heterogeneous conversion of naphthalene. *Fuel Process. Technol.* 172 (2018) 125–132
- [20] H. Marsh, F. Rodriguez-Reinoso, *Activated Carbon*, Elsevier, Oxford, 2006.
- [21] F. Nestler, L. Burhenne, M.J. Amentbrink, T. Aicher. Catalytic decomposition of biomass tars: the impact of wood char surface characteristics on the catalytic performance for naphthalene removal, *Fuel Process. Technol.* 145 (2016) 31–41.
- [22] Y. Song, Y. Wang, X. Hu, J. Xiang, S. Hu, D. Mourant, T. Li, L. Wu, C.Z. Li. Effects of volatile-char interactions on in-situ destruction of nascent tar during the pyrolysis and gasification of biomass. Part II. Roles of steam, *Fuel* 143 (2015) 555–562.
- [23] D. Feng, Y. Zhao, Y. Zhang, S. Sun, S. Meng, Y. Guo, Y. Huang. Effects of K and Ca on reforming of model tar compounds with pyrolysis biochars under H₂O or CO₂, *Chem. Eng. J.* 306 (2016) 422–432.
- [24] D. Feng, Y. Zhao, Y. Zhang, J. Gao, S. Sun. Changes of biochar physiochemical structures during tar H₂O and CO₂ heterogeneous reforming with biochar, *Fuel Process. Technol.* 165 (2017) 72–79.
- [25] D. Feng, Y. Zhang, Y. Zhao, S. Sun, J. Gao. Improvement and maintenance of biochar catalytic activity for in-situ biomass tar reforming during pyrolysis and H₂O/CO₂ gasification. *Fuel Process. Technol.* 172 (2018) 106–114
- [26] C. Choi, K. Shima, S. Kudo, K. Norinaga, X. Gao, J-I Hayashi. Continuous monitoring of char surface activity towards benzene, *Carbon Resources Conversion.* 2 (2019) 43–50.
- [27] A. Korus, A. Samson, A. Szlek, A. Katelbach-Wozniak, S. Śladek, *Pyrolytic toluene conversion to benzene and coke over activated carbon in a fixed-bed reactor*, *Fuel* 207 (2017) 283–292.
- [28] Y-L Zhang, Y-H Luo, W-G Wu, S-H Zhao, Y-F Long. Heterogeneous cracking reaction of tar over biomass char, using naphthalene as model biomass tar, *Energy Fuels* 28 (2014) 3129–3137.
- [29] G. Ravenni, O.H. Elhami, J. Ahrenfeldt, U.B. Henriksen, Y. Neubauer. Adsorption and decomposition of tar model compounds over the surface of gasification char and active carbon within the temperature range 250–800 °C, *Appl. Energy* 241 (2019) 139–151
- [30] M. Morin, X. Nitsch, M. Hémati. Interactions between char and tar during the steam gasification in a fluidized bed reactor, *Fuel* 224 (2018) 600–609.
- [31] Y. Zhang, S. Kajitani, M. Ashizawa, Y. Oki. Tar destruction and coke formation during rapid pyrolysis and gasification of biomass in a drop-tube furnace, *Fuel* 89 (2010) 302–309.
- [32] D. Buentello-Montoya, X. Zhang, S. Marques, M. Geron. Investigation of competitive tar reforming using activated char as catalyst, *Energy Procedia* 158 (2019) 828–835
- [33] J. Karl, T. Pröll. Steam gasification of biomass in dual fluidized bed gasifiers: A review, *Renew. Sust. Energ. Rev.* 98 (2018) 64–78
- [34] *Guideline for sampling and analysis of tar and particles in biomass producer gases*. ECN 2002. ECN-C-02-090.
- [35] van Paasen SVB. *Tar formation in a fluidised-bed gasifier. Impact of fuel properties and operating conditions*. 2004. ECN-C-04-013.
- [36] D. Fuentes-Cano, A. Gomez-Barea, S. Nilsson. generation and secondary conversion of volatiles during devolatilization of dried sewage sludge in a fluidized bed. *Ind. Eng. Chem. Res.* 52 (2013) 1234–1243.
- [37] L. Jiang, S. Hu, J. Xiang, S. Su, L. Sun, K. Xu, Y. Yao. Release characteristics of alkali and alkaline earth metallic species during biomass pyrolysis and steam gasification process. *Bioresour. Technol.* 116 (2012) 278–284
- [38] A. Dieguez-Alonso, A. Funke, A. Anca-Couce, A. G. Rombolà, G. Ojeda, J. Bachmann, F. Behrendt. Towards biochar and hydrochar engineering—influence of process conditions on surface physical and chemical properties, thermal stability, nutrient availability, toxicity and wettability, *Energies.* 11 (2018) 496